Acta Cryst. (1976). B**32**, 1083

A Powder Neutron and X-ray Diffraction Determination of the Structure of $Ba_3Ta_2ZnO_9$: an Investigation of Perovskite Phases in the System Ba–Ta–Zn–O and the Preparation of $Ba_2TaCdO_{5\cdot5}$ and $Ba_2CeInO_{5\cdot5}$

By A. J. Jacobson, B. M. Collins and B. E. F. Fender

*Inorganic Chemistry Laboratory, South Parks Road, Oxford OX*1 3*QR*, *England*

(*Received* 8 *September* 1975; *accepted* 12 *September* 1975)

The long-range order of Ta–Zn in $Ba_3Ta_2ZnO_9$ has been demonstrated by X-ray diffraction and the structure refined by profile analysis of powder neutron diffraction data. Accurate metal–oxygen distances are provided and the Zn–O distance (1·98 Å) is considerably smaller than would be expected from the sum of normal ionic radii. The Ta–O distances are, on the other hand, larger than those found in similar oxygen perovskites. The phases $Ba_2TaMO_{5\cdot5}$ (M = Zn, Cd) and $Ba_2CeInO_{5\cdot5}$ have also been prepared but only $Ba_2TaZnO_{5\cdot5}$ shows evidence of any cation ordering.

Introduction

An unusual feature of the ABO_3 perovskite and related structures is that the B sites may simultaneously accommodate a wide range of cations which differ in formal charge. For stoichiometric oxide systems of the type $A(B,B')O_3$ where A is divalent, the average B site charge is 4+ and the B and B′ cations may or may not be ordered depending on differences in their charges and radii. In general, for charge differences ≥ 4 the cations order but when the charges differ by less than 4 disordered structures are found unless there is a large difference in radii. For example, Ba_2NbFeO_6 is disordered (Galasso & Darby, 1962; $Nb^{5+} = 0\cdot64$, $Fe^{3+} = 0\cdot64$ Å) whereas Ba_2NbInO_6 is ordered (Brixner, 1960; $In^{3+} = 0\cdot79$ Å). Madelung energy calculations have been made for a number of systems (Rosenstein & Schor, 1963) and suggest that the electrostatic ordering energy increases with the square of the charge difference.

The particular AO_3 stacking sequence and the B cation distribution is often determined by size effects; *e.g.* Ba_2TaYO_6 and Ba_2TaCrO_6 have cubic and 6*H* structures respectively but in other cases, *e.g.* 5*H* $Ba_5Ta_4O_{15}$ and 6*H* $Ba_3Ru_2MgO_9$, additional influences such as cation repulsion or metal–metal bonding may play a significant part. In addition to the stoichiometric phases, Sabatier, Wathlé, Besse & Baud (1971) prepared several compounds of general composition $A_2BB'O_{5\cdot5}$ which have ordered 6+ and 1+ cations on a double cubic cell. Several other systems of this type where $B = Ca^{2+}, Sr^{2+}$ or Ba^{2+}: and $B' = Nb^{5+}, Ta^{5+}$ and Pa^{5+} have also been reported (Galasso, Katz & Ward, 1959; Galasso & Darby, 1962; Keller & Wassilopulos, 1965) but the degree of cation ordering is not known. All the anion-deficient phases have low values of the tolerance factor, $0\cdot85 < t < 0\cdot99$ but no structural distortions have been observed.

Most reported examples of B cation ordering correspond to the general stoichiometries $A_2BB'O_6$ and $A_3B_2B'O_9$ [see, *e.g.* Goodenough & Longo (1970)]. Although $A_2BB'O_6$ compounds have been extensively studied no detailed structural investigation of an ordered $A_3B_2B'O_9$ system has been reported, though it should be noted that not all examples where B:B′ is 2:1 lead to genuine 2:1 ordering; some behave as 1:1 systems, *e.g.* $Ba_3Fe_2UO_9$ corresponds to $Ba_2Fe(U_{2/3}Fe_{1/3})O_6$ (Padel, Poix & Michel, 1972).

In the present work we have carried out a combined neutron and X-ray study of $Ba_3Ta_2ZnO_9$ to investigate the Ta–Zn ordering and to determine accurately the local O environment of the two B cations. We have also explored the possibility of forming anion-deficient and anion-excess perovskites in the Ba–Ta–Zn–O system.

A summary of 2:1 phases containing Ta and Nb is given in Table 1. The *c*/*a* ratio refers to a hexagonal cell with *c* corresponding to the body diagonal of the cubic cell and is ideally $\sqrt{3}/\sqrt{2} = 1\cdot2247$. For compounds with *t* slightly greater than 1, only small deviations from this value are found, but, for $t < 0\cdot99$, *c*/*a* increases rapidly.

Table 1. $Ba_3B_2^{5+}B'^{2+}O_9$ *compounds**

(All have the 6*C* doubled cubic structure unless otherwise stated)

	B = Ta (0·64 Å)			B = Nb (0·64 Å)	
B′	Å	*t*	*c*/*a*	*t*	*c*/*a*
Mg	0·72	1·03	1·222	1·03	1·227
Ni	0·70	1·03	1·225	Simple cubic	
Co	0·735	1·02	1·226	Simple cubic	
Zn	0·745	1·02	1·227	Simple cubic	
Mn	0·82	1·01	1·225	—	
Ca	1·00	0·98	1·236	0·98	1·225
Sr	1·16	0·96	1·256	—	
Ba	1·36	0·93	1·320	0·93	1·331

* See Goodenough & Longo (1970)

Experimental

Preparation of samples

The starting materials used, $BaCO_3$, Ta_2O_5, ZnO, were obtained from Johnson Matthey 'Specpure' chemicals. All oxides were dried in O_2 before use and the $BaCO_3$ was fired at 900 °C under CO_2. Stoichiometric starting mixtures were weighed on an analytical balance and hand ground in an agate mortar. Reactions were carried out in sintered alumina crucibles in air.

Six compositions, $Ba_{12}Ta_{12-x}Zn_xO_y$ with $x = 2$, 3, 4, 5, 6, and 7, were studied. The appropriate starting mixtures were fired at 1150 °C (96 h) with two intermediate regrinds and at 1350 °C (120 h) with one regrind. No reaction with the crucibles was observed. The samples came to constant weight after the 1150 °C firing and were all white. Only two compositions gave single phase products (see below) and their thermogravimetric compositions were $Ba_{12}Ta_8Zn_4O_{35·96(4)}$ and $Ba_{12}Ta_6Zn_6O_{33·05(10)}$. Two analogous compounds $Ba_{12}Ta_6Cd_6O_{33·00(5)}$ and $Ba_{12}Ce_6In_6O_{32·98(5)}$ were prepared by similar methods as appropriate with CdO, CeO_2 and In_2O_3 (also supplied by Johnson Matthey Chemicals Ltd) as starting oxides.

Table 2. $Ba_3Ta_2ZnO_9$: 1350 °C *ordered phase X-ray data*

h k l	*I*(obs)	*I*(cal)	*d*(obs)	*d*(cal)
0 0 1	1·0	1·0	7·07	7·10
1 0 0	3·0	3·0	5·00	5·01
1 0 1	4·3	4·0	4·09	4·09
0 0 2	0·6	0·4	3·549	3·552
1 1 0 1 0 2	100·0	105·0	2·890	2·890 2·897
1 1 1	0·8	0·8	2·676	2·677
2 0 0	0·5	0·6	2·501	2·503
2 0 1 0 0 3	2·3	2·1	2·360	2·361 2·368
1 1 2	1·2	1·1	2·238	2·242
1 0 3	0·8	1·1	2·139	2·141
2 0 2	30·6	29·1	2·045	2·046
2 1 0	0·3	0·6	1·891	1·892
2 1 1 1 1 3	1·9	0·3	1·828	1·828 1·832
0 0 4	0·6	0·1	1·776	1·776
2 0 3	0·8	0·7	1·720	1·720
1 0 4	38·3	38·8	1·674	1·674
3 0 0 2 1 2	0·5	0·4	1·669	1·669 1·670
2 0 4 2 2 0	18·2	16·4	1·448 1·445	1·448 1·445
2 1 4 3 1 2	16·6	15·6	1·294	1·295 1·293
2 0 5 2 2 3 4 0 1	0·6	0·3	1·234	1·236 1·233 1·232
3 1 3	0·4	0·3	1·1975	1·1977
0 0 6 4 0 2	6·2	5·1	1·1836 1·1801	1·1840 1·1803
3 2 1 2 1 5	0·2	0·1	1·1337	1·1337 1·1361
1 1 6 3 1 4 3 2 2 4 1 0	23·7	24·1	1·0934	1·0956 1·0938 1·0927 1·0923
3 0 5 4 1 1	0·8	1·0	1·0818	1·0817 1·0796
4 0 4	3·1	2·9	1·0228	1·0230
0 0 7 2 2 5	0·3	0·6	1·0129	1·0148 1·0131
3 0 6 3 2 4 5 0 2 3 3 0	13·8	13·8	0·9646	0·9656 0·9643 0·9636 0·9633
2 2 6 4 2 2	12·1	11·5	0·9157 0·9140	0·9158 0·9141
2 1 7 3 2 5 5 1 1	0·6	0·7	0·8945	0·8943 0·8931 0·8919
1 0 8 5 0 4 5 1 2	9·5	9·6	0·8744 0·8718	0·8743 0·8721 0·8716
3 0 7 4 1 5	0·5	0·6	0·8658	0·8671 0·8660
2 0 8 4 2 4 6 0 0	15·6	16·0	0·8370 0·8349	0·8369 0·8349 0·8343

X-ray diffraction patterns of the compounds were taken with a Philips high-angle goniometer and Cu $K\alpha$ radiation.

$Ba_3Ta_2ZnO_9$

The products obtained from both the 1150 °C and 1350 °C firings were examined. The former was indexed on a simple cubic cell with $a = 4·091$ (1) Å; the latter was hexagonal with $a = 5·780$ (1), $c = 7·104$ (1) Å (see Table 2). The hexagonal lattice parameters are in good agreement with those obtained by Galasso & Pyle (1963) but the c/a ratio of 1·229 is slightly larger than their value of 1·227.

Neutron diffraction

In order to examine in greater detail the local **B** cation environment of the hexagonal phase of $Ba_3Ta_2ZnO_9$, neutron diffraction data were collected at 4·2 K on a powder diffractometer at UKAEA Harwell. A wavelength of 1·540 Å from the (511) planes of a Ge monochromator was used and data were collected in the range $10° < 2\theta < 101°$. The structural parameters were refined with the whole data set by the profile method (Rietveld, 1967). The scattering lengths used were $b_{Ba} = 0·52$, $b_{Ta} = 0·70$, $b_{Zn} = 0·57$ and $b_O = 0·58 \times 10^{-12}$ cm (Neutron Diffraction Commission, 1972). The starting parameters for the model based on $P\bar{3}m1$ correspond to ideally close-packed BaO_3 layers but because of the similarity in scattering lengths of Ta and Zn, the data are not sensitive to the TaZn distribution and these occupation numbers were fixed at the values corresponding to the fully ordered model, *i.e.* Ta in 2(*d*) and Zn in 1(*b*) as indicated by the X-ray data (see below). The neutron Bragg intensities were refined until all parameter shifts were less than $0·3\sigma$. The final profile R value was 8·3 % which corresponds to a value of 4·3 % based on integrated intensities. The observed and calculated profiles are shown in Fig. 1, the atomic positional parameters in Table 3, and interatomic distances and angles in Table 4. The local **B** cation environment is illustrated in Fig. 2.

X-ray diffraction

X-ray intensities for the hexagonal structure were also refined in $P\bar{3}m1$ with the same starting parameters as in the neutron refinement. The X-ray measurements were made at room temperature. An overall temperature factor of 1 Å^2 was assumed and the data refined until all parameter shifts were again less than 0·3σ. A final R, based on integrated intensities, of 6·4% was obtained. The results are given in Table 3. The occupation numbers were in good agreement with the postulated fully ordered model, although the precision of the measurements gives results which are not incompatible with a small amount of disorder.

Table 3. *Atomic positional parameters for* $Ba_3Ta_2ZnO_9$ *from X-ray and neutron refinements*

$Ba_3Ta_2ZnO_9$	$P\bar{3}m1$	X-rays		
		x	y	z
Ba(1)	$2d$	$\frac{1}{3}$	$\frac{2}{3}$	0·688 (4)
Ba(2)	$1a$	0	0	0
Ta	$2d$	$\frac{1}{3}$	$\frac{2}{3}$	0·169 (4)
Zn	$2b$	0	0	$\frac{1}{2}$
O(1)	$3e$	$\frac{1}{2}$	0	0
O(2)	$6i$	0·164 (2)	0·328 (4)	0·347 (2)
	Occupation numbers		Ta	2·02 (9)
			Zn	1·03 (11)
	R(intensities)		6·4 %	

$Ba_3Ta_2ZnO_9$	$P\bar{3}m1$	Neutrons
Ba(1)	z	0·6783 (11)
Ta	z	0·1609 (8)
O(2)	x	0·1644 (8)
	z	0·3457 (5)

Overall temperature factor B 0·20 (3) Å^2

R(profile) 8·3 %

R(intensities) 4·3 %

Table 4. *Interatomic distances and angles in* $Ba_3Ta_2ZnO_9$ *from the neutron diffraction data*

Ba(1)–O(1)	2·830 (8) Å	O(1)–O(1)	2·890 (1) Å
Ba(1)–O(2)	2·895 (12)	O(1)–O(2)	2·976 (4)
Ba(1)–O(2)	2·906 (12)	O(2)–O(2)	2·851 (8)
Ba(2)–O(1)	2·890 (1)	O(2)–O(2)	2·741 (8)
Ba(2)–O(2)	2·956 (4)	Ta—O(1)	2·023 (7)
Zn—O(2)	1·977 (4)	Ta—O(2)	2·141 (10)
O(2)-Zn-O(2)	92·2 (5)°	O(1)-Ta-O(1)	91·2 (4)°
O(2)-Zn-O(2)	87·8 (5)	O(1)-Ta-O(2)	91·1 (6)
		O(2)-Ta-O(2)	83·4 (8)

Intensities were calculated for the cubic phase assuming space group $Pm3m$, ideal close-packing of the BaO_3 layers and a disordered distribution of Ta and Zn on the B sites. An overall temperature factor of 1·0 Å^2 was used and the observed and calculated intensities were in good agreement.

$Ba_2TaZnO_{5.5}$

The X-ray pattern of the 1150°C product was completely indexed on a simple cubic cell with a_o= 4·091 (1) Å. Moreover, unlike $Ba_3Ta_2ZnO_9$, the sample heated to 1350°C showed no obvious ordering effects and the intensities were identical to the 1150°C sample. However, long-exposure Debye–Scherrer photographs indicated the presence of two very weak reflexions with d=4·720 and 2·469 Å corresponding to the 111 and 311 reflexions of a doubled cubic unit cell with a_o=8·183 Å indicative of a small amount of long range Ta–Zn ordering. The observed and calculated intensities for the 1150°C (and 1350°C) sample are, however, still in good agreement with a disordered model.

Other Ta–Zn compositions

All other Ta:Zn ratios gave products which were at least two-phase mixtures. The oxygen deficient $Ba_{12}Ta_5Zn_7O_{31.5}$ and $Ba_{12}Ta_7Zn_5O_{34.5}$ gave two-phase mixtures of the 1:1 and 2:1 Ta:Zn compounds. In the 1:1 Ta:Zn compound, however, four weak extra lines

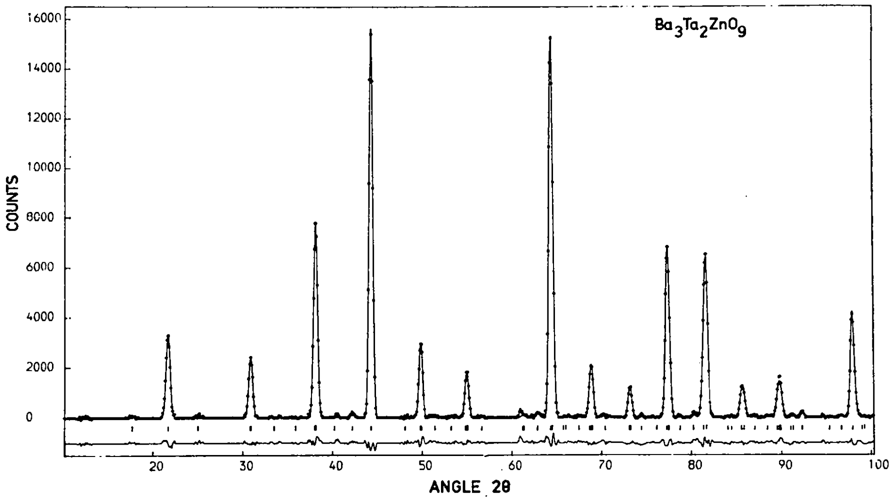

Fig. 1. Powder neutron diffraction profile for $Ba_3Ta_2ZnO_9$. Small circles are the experimental points and the continuous line passes through the calculated profile. The small vertical lines are the calculated *hkl* positions and the bottom trace is a difference plot.

were observed which could not be indexed on any supercell. The oxygen excess $Ba_{12}Ta_9Zn_3O_{37\cdot5}$ and $Ba_{12}Ta_{10}Zn_2O_{39}$ gave lines corresponding to $Ba_5Ta_4O_{15}$ and either ordered or disordered $Ba_3Ta_2ZnO_9$ depending on the temperature of preparation. No simple combination of $Ba_5Ta_4O_{15}$ and $Ba_3Ta_2ZnO_9$ can account for the total stoichiometry and consequently it is likely that some starting oxides are also present in small amounts.

$Ba_2TaCdO_{5\cdot5}$ and $Ba_2CeInO_{5\cdot5}$

The 1150 °C and 1350 °C products of $Ba_2TaCdO_{5\cdot5}$ and $Ba_2CeInO_{5\cdot5}$ could both be indexed on simple cubic cells with lattice parameters of 4·168 (1) and 4·320 (1) Å respectively. No super-lattice lines due to cation ordering were detectable either in diffractometer traces or in long-exposure Debye–Scherrer photographs. The observed and calculated intensities for the cation disordered models were in good agreement.

Discussion

The long-range cation ordering observed in $Ba_3Ta_2ZnO_9$ appears at first sight to originate in the difference in the ionic size of the two cations; $Ta^{5+} = 0\cdot64$, $Zn^{2+} = 0\cdot74$ Å (Shannon & Prewitt, 1969). However, examination of the observed metal–oxygen distances shows that these distances are unexpected in the light of the normal ionic radii. Thus the average Ta–O distance (2·08 Å) is longer than that found in either $Ba_5Ta_4O_{15}$ (2·005 Å, Shannon & Katz, 1970) or $Ba_4Ta_3LiO_{12}$ (Collins, Jacobson & Fender, 1974) whereas the Zn–O distance is much shorter than would be expected from the sum of the ionic radii. The reverse of the expected effects is clearly seen where Zn and Ta compete for the same corner-sharing O atom; the Zn–O distance = 1·98 Å ($Zn^{2+} + O^{2-} = 2\cdot09$ Å) and the O–Ta distance 2·14 Å ($Ta^{5+} + O^{2-} = 1\cdot99$ Å). There is no obvious simple explanation. It is conceivable however that the high electron affinity of Ta^{5+} (and considerable covalence in the Ta–O bond) modifies the O ligand field so that some 3*d* electron donation becomes possible from Zn to O (in effect into a bond arising from Ta–O overlap). Combined with back donation from O to the *s–p* orbitals of Zn this could give rise to an abnormally high Zn–O covalence and a correspondingly short distance. The effect of delocalizing the *d* electrons of Zn would be to transfer electron density to the *d*-orbital antibonding regions of Ta thus weakening the bonding and increasing the Ta–O distance observed. The reduced contribution to the lattice energy from an overall increase in the Ta–O distance is partially compensated in a familiar way by an off-centre Ta displacement which leads to three short and three long bonds with O (*cf.* cubic $BaTiO_3$).

Removal of O from $Ba_3Ta_2ZnO_9$ appears to weaken the tendency for B-cation ordering as only partial long-range order is found in $Ba_2TaZnO_{5\cdot5}$. The Ta:Zn ratio has of course been altered as well and it is plausible that the reduction in the average potential on the B-cation site (and on the anion site) is the cause of diminished ordering. It is probable that thermodynamic equilibrium has been reached because the presence of O vacancies would be expected to assist the B-cation diffusion which is rapid enough at 1350 °C to establish complete ordering in the stoichiometric compound. $Ba_2TaCdO_{5\cdot5}$ and $Ba_2CeInO_{5\cdot5}$ also appear to be disordered. In the latter, disorder would be predicted because the difference in the B-cation charges is only 1+. For $Ba_2TaCdO_{5\cdot5}$ the nominally greater difference in cation size suggests that ordering would be more likely than in $Ba_2TaZnO_{5\cdot5}$. No sign of ordering was in fact observed and though the X-ray examination is less sensitive in this case (a neutron study is ruled out by the high absorption of Cd) if any long-range order does occur it must be small. This result and consideration of the earlier discussion of $Ba_3Ta_2ZnO_9$ suggests that the effective sizes of Cd^{2+} and Ta^{5+} in $BaTaCdO_{5\cdot5}$ may be little different.

Finally we note that decreasing the Zn content does not lead to the formation of anion-excess phases, even though the replacement of Zn^{2+} by Ta^{5+} appears to meet one of the criteria for the formation of such phases, *i.e.* a reduction in B-cation radius as for example in $LaMnO_{3+x}$ where the radius of Mn^{4+} is 16% smaller than the Mn^{3+} ion it replaces (Tofield & Scott, 1975). In the present case we have shown, however, that the normal radii may be inappropriate and there is also competition from the stable $Ba_5Ta_4O_{15}$ phase.

We are grateful to the Science Research Council and AERE Harwell for the provision of neutron facilities. One of us (B.M.C.) thanks AERE for the provision of a studentship.

References

BRIXNER, L. H. (1960). *J. Phys. Chem.* **64**, 165–166.
COLLINS, B. M., JACOBSON, A. J. & FENDER, B. E. F. (1974). *J. Solid State Chem.* **10**, 29–35.
GALASSO, F. & DARBY, W. (1962). *J. Phys. Chem.* **66**, 131–132.

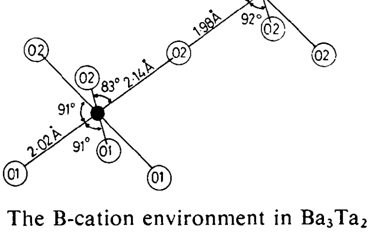

Fig. 2. The B-cation environment in $Ba_3Ta_2ZnO_9$.

GALASSO, F., KATZ, L. & WARD, R. (1959). *J. Amer. Chem. Soc.* **81**, 820–823.

GALASSO, F. & PYLE, J. (1963). *Inorg. Chem.* **2**, 482–484.

GOODENOUGH, J. B. & LONGO, J. M. (1970). *Landolt-Börnstein. Crystallographic and Magnetic Properties of Perovskite and Perovskite Related Compounds*, New Series, Group III, Vol. 4a. New York: Springer-Verlag.

KELLER, C. & WASSILOPULOS, W. (1965). *Radiochim. Acta*, **5**, 87–91.

NEUTRON DIFFRACTION COMMISSION (1972). *Acta Cryst.* A**28**, 357–358.

PADEL, L., POIX, P. & MICHEL, A. (1972). *Rev. Chem. Min.* **9**, 337–350.

RIETVELD, H. M. (1967). *Acta Cryst.* **22**, 151–152.

ROSENSTEIN, R. D. & SCHOR, R. (1963). *J. Chem. Phys.* **38**, 1789–1790.

SABATIER, R., WATHLÉ, M., BESSE, J.-P. & BAUD, G. (1971). *J. Inorg. Nucl. Chem.* **33**, 1597–1613.

SHANNON, J. & KATZ, L. (1970). *Acta Cryst.* B**26**, 102–105.

SHANNON, R. D. & PREWITT, C. T. (1969). *Acta Cryst.* B**25**, 925–946.

TOFIELD, B. C. & SCOTT, W. R. (1974). *J. Solid State Chem.* **10**, 183–194.

Acta Cryst. (1976). B**32**, 1087

A Powder Neutron Diffraction Study of the Structure of and Oxygen Vacancy Distribution in 6*H* $BaFeO_{2.79}$

BY A. J. JACOBSON

Inorganic Chemistry Laboratory, South Parks Road, Oxford OX1 3QR, England

(*Received* 8 *September* 1975; *accepted* 12 *September* 1975)

The structure and oxygen vacancy distribution have been determined for 6*H* $BaFeO_{2.79}$. The hexagonally stacked AO_3 layers are found to have composition $BaO_{2.5}$ while the cubic stacked layers are $BaO_{2.835}$. Possible models for the vacancy distribution are discussed in relation to the defect structures of $SrFeO_{2.5}$ and $SrFeO_{2.75}$.

Introduction

The anion deficient perovskite related compounds ABO_{3-x} where A = Sr, Ba and B = Mn, Co, Ni have structures which may be described as close packed AO_3 layers with B cations in octahedral sites (Katz & Ward, 1964). All show extensive non-stoichiometry in the range $0<x<0.5$ but considerable differences are found in the structures and compositions of intermediate phases. Little is known of the detailed distribution of O vacancies.

The $BaFeO_{3-x}$ system is one of the most extensively investigated, in part because of the interesting magnetic properties which result from the presence of both Fe^{3+} and Fe^{4+}. Gallagher, MacChesney & Buchanan (1965) and MacChesney, Potter, Sherwood & Williams (1965) identified two phases; $BaFeO_{2.5}$, thought to be isostructural with brownmillerite and a hexagonal phase $BaFeO_{2.84-2.95}$. Subsequently, Mori (1965, 1966, 1970) reported the phase at $x = 0.5$ to be triclinic and in addition prepared a number of other compounds including a second triclinic phase, $BaFeO_{2.67}$, rhombohedral $BaFeO_{2.62-2.64}$, tetragonal $BaFeO_{2.75-2.81}$ and 6*H* hexagonal $BaFeO_{2.63-2.95}$. All compounds other than triclinic *I* and 6*H* were obtained at low temperatures and showed weak superlattice reflexions in their powder X-ray patterns. Zanne & Gleitzer (1971) found that the 6*H* hexagonal phase exists in the range $BaFeO_{2.95}$–$BaFeO_{2.69}$ and in addition reported a 12*R* compound with a BaO_3 stacking sequence *chhc*, prepared at high O_2 pressure. The twelve-layer modification has also been described by Takeda, Shimada, Kanamaru & Koizumi (1973).

Phase relations in nonstoichiometric perovskite related compounds are often complicated by slow diffusion of metal ions which may lead to the formation of metastable phases with respect to the cation distribution. Equilibrium with respect to O is generally attained more rapidly. Ichida (1973) investigated the attainment of equilibrium by using the decomposition of $BaFeO_4$ as a synthetic route in preference to the more usual solid state reaction of Fe_2O_3 with $BaCO_3$ or BaO_2. Triclinic *I* and 6*H* $BaFeO_{2.63-2.95}$ were established as equilibrium phases and in addition to the low-temperature phases of Mori a new $BaFeO_{2.5}$ structure was reported.

In the present work, the structure and O vacancy distribution of 6*H* $BaFeO_{2.79}$ have been determined by powder neutron diffraction. No detailed structures for any of the phases discussed have been reported, unlike the analogous $BaMnO_{3-x}$ system where the structures of the 8*H* compound and the structure and vacancy distribution in 4*H* $Ba_{0.5}Sr_{0.5}MnO_{2.83}$ have been determined (Potoff, Chamberland & Katz, 1973; Jacobson & Horrox, 1976). In the Fe system the effect of a different preferred coordination for the reduced cation is expected to lead to a different vacancy distribution.